HHS Public Access

Author manuscript

Biochim Biophys Acta. Author manuscript; available in PMC 2017 January 22.

Published in final edited form as:

Biochim Biophys Acta. 2016 September ; 1860(9): 1884–1897. doi:10.1016/j.bbagen.2016.05.037.

Gamma-irradiation produces active chlorine species (ACS) in physiological solutions: Secoisolariciresinol diglucoside (SDG) scavenges ACS - A novel mechanism of DNA radioprotection

Om P. Mishra[a,1], **Anatoliy V. Popov**[b,1], **Ralph A. Pietrofesa**[a], and **Melpo Christofidou-Solomidou**[a,*]

[a]Department of Medicine, Pulmonary, Allergy and Critical Care Division, University of Pennsylvania Perelman School of Medicine, Philadelphia, PA 19104, United States

[b]Department of Radiology, University of Pennsylvania Perelman School of Medicine, Philadelphia, PA 19104, United States

Abstract

Background—Secoisolariciresinol diglucoside (SDG), the main lignan in whole grain flaxseed, is a potent antioxidant and free radical scavenger with known radioprotective properties. However, the exact mechanism of SDG radioprotection is not well understood. The current study identified a novel mechanism of DNA radioprotection by SDG in physiological solutions by scavenging active chlorine species (ACS) and reducing chlorinated nucleobases.

Methods—The ACS scavenging activity of SDG was determined using two highly specific fluoroprobes: hypochlorite-specific 3′-(*p*-aminophenyl) fluorescein (APF) and hydroxyl radical-sensitive 3′-(*p*-hydroxyphenyl) fluorescein (HPF). Dopamine, an SDG structural analog, was used for proton ^{1}H NMR studies to trap primary ACS radicals. Taurine *N*-chlorination was determined to demonstrate radiation-induced generation of hypochlorite, a secondary ACS. DNA protection was assessed by determining the extent of DNA fragmentation and plasmid DNA relaxation following exposure to ClO^- and radiation. Purine base chlorination by ClO^- and γ-radiation was determined by using 2-aminopurine (2-AP), a fluorescent analog of 6-aminopurine. Results: Chloride anions (Cl^-) consumed >90% of hydroxyl radicals in physiological solutions produced by γ-radiation resulting in ACS formation, which was detected by ^{1}H NMR. Importantly, SDG scavenged hypochlorite- and γ-radiation-induced ACS. In addition, SDG blunted ACS-induced fragmentation of calf thymus DNA and plasmid DNA relaxation. SDG treatment before or after ACS exposure decreased the ClO^- or γ-radiation-induced chlorination of 2-AP. Exposure to γ-radiation resulted in increased taurine chlorination, indicative of ClO^- generation. NMR studies revealed formation of primary ACS radicals (chlorine atoms ($Cl^{\bullet}$) and dichloro radical anions ($Cl_2^{-\bullet}$)), which were trapped by SDG and its structural analog dopamine.

*Corresponding author at: Department of Medicine, Pulmonary, Allergy, and Critical Care Division, University of Pennsylvania Perelman School of Medicine, 3450 Hamilton Walk, Edward J. Stemmler Hall, 2nd Floor, Office Suite 227, Philadelphia, PA 19104, United States.

[1]The first two authors have contributed equally to this work.

Transparency document

The Transparency document associated with this article can be found in online version.

Conclusion—We demonstrate that γ-radiation induces the generation of ACS in physiological solutions. SDG treatment scavenged ACS and prevented ACS-induced DNA damage and chlorination of 2-aminopurine. This study identified a novel and unique mechanism of SDG radioprotection, through ACS scavenging, and supports the potential usefulness of SDG as a radioprotector and mitigator for radiation exposure as part of cancer therapy or accidental exposure.

Keywords

Active chlorine species; 2-Aminopurine; Chlorine atoms; Dichloro radical anion; DNA fragmentation; Hydroxyl radical; Hypochlorite ion; γ-Radiation; Mitigation; Radicals; Radioprotection; Secoisolariciresinol diglucoside; Taurine chloramine

1. Introduction

Active chlorine species (ACS) include chlorine-containing molecules in oxidation states other than −1. In physiological solutions, ACS are represented by molecules in oxidation states 0 and +1, namely, chlorine atoms ($Cl^{\bullet}$), chlorine molecules (Cl_2), dichloro radical anions ($Cl_2^{\bullet-}$) hypochlorous acid (HOCl) and hypochlorite anions (ClO^-), which are formed by the oxidation of chloride anion Cl^- [1–7]. Among these ACS HOCl (ClO^-), a potent oxidant, can be produced in vivo by neutrophils containing activated myeloperoxidase which catalyzes the reaction between physiologically present chloride ions and hydrogen peroxide (H_2O_2) [8]. In addition to neutrophils, eosinophils are also capable of generating HOCl, from H_2O_2 and Cl^-, by using eosinophil peroxidase. However, Cl^- is not a preferred substrate in vivo [9,10]. At physiological pH, a mixture of both HOCl and ClO^- exists. HOCl kills microorganisms by oxidative damage. However, excessive production of HOCl is also known to cause inflammation and tissue damage. Hypochlorite modifies adenine nucleotides resulting in the formation of chloramines, which are implicated in neutrophil-mediated toxicity [11–13].

HOCl and its conjugated base ClO^- oxidize amino acids, peptides, proteins and lipids [14–17], and chlorinate bases in cellular DNA and RNA [14,18,19]. The reaction of HOCl/ClO^- results in the modification of both purine and pyrimidine nucleotides at the endocyclic –NH groups of guanine and thymine as well as the exocyclic NH_2 groups of guanine, adenine and cytosine derivatives [20,21] resulting in the formation of chloramines such as RNHCl and RR'NCl. The primary modified bases include 5-chlorocytosine, 8-chloroadenine and 8-chloroguanine in DNA and RNA [19,22].

It is well known that γ-radiation is capable of ionizing atoms and molecules. In biological systems or in solution, ionizing radiation generates hydroxyl radicals ($^{\bullet}OH$) [23–25], which are believed to be the source of ionizing radiation-induced damage to cellular components, including lipids, proteins and DNA [26,27]. However, these highly unstable hydroxyl radicals can be scavenged by Cl^- ions which are present at very high concentrations in physiological medium. This leads to generation of ACS [28–31], among which relatively stable ClO^- was suggested as the radiation-derived toxicant [28]. The pivotal role of ACS in hydroxyl radical-mediated chemical processes such as electrolysis [1,32–37] and Fenton

reaction [38], is well known. However, the novel role of ACS, especially Cl•, $Cl_2^{\bullet -}$ and Cl_2, in γ-radiation-induced damage has only been suggested in one publication [30]. The current manuscript is to shed light on the production of ACS in physiological solutions following γ-radiation and its role in radiation-induced DNA damage. In chloride-containing solutions, ACS are formed as products of radiolysis and can impair physiological functions [31]. Therefore, we propose that radiation–induced DNA damage is mediated, in part, by radiation-generated ACS.

We have recently chemically synthesized two diastereomers of secoisolariciresinol diglucoside (SDG) [39], shown to be equipotent in their antioxidant, free radical scavenging and DNA protective properties [39,40]. The present study evaluates SDG in DNA radioprotection from γ-radiation-induced generation of ACS in physiological saline solutions using novel and specific probes. Hypochlorite-specific 3′-(*p*-aminophenyl) fluorescein (APF) and hydroxyl radical-sensitive 3′-(*p*-hydroxyphenyl) fluorescein (HPF) provide greater specificity and reproducibility for determining reactive oxygen (ROS) and chlorine species by fluorescence [41]. Dopamine, a simplified structural analog of SDG, was used to distinguish radical chlorination from hypochlorite-mediated oxidative chlorination [42] by proton magnetic resonance (^{1}H NMR) and taurine was used to detect hypochlorite-mediated *N*-chlorination.

2. Materials and methods

2.1. Chemicals

ROS indicator probes APF and HPF, plasmid DNA (pBR322), ethidium bromide, ultrapure 10X TAE buffer and 1 kb plus DNA ladder were purchased from Invitrogen (Life Technologies, Carlsbad, CA). Sodium hypochlorite, silibinin, quercetin, L-methionine, agarose (ultrapure) and calf thymus DNA were purchased from Sigma-Aldrich (St. Louis, MO). Hypochlorite concentration was documented spectrophotometrically in 10 mM NaOH at pH 12 using molar coefficient at 292 nm (ε_{292} = 350 M^{-1} cm^{-1}). Dulbecco's phosphate buffered saline (DPBS ×1, 21-031-CV) without calcium and magnesium was purchased from Mediatech Inc. (Manassas, VA). Commercially available SDG (com) was purchased from Chromadex (Irvine, CA) and synthetic SDGs (SDG (*S,S*) and SDG (*R,R*)) were synthesized by our group [39].

2.2. Determination of hypochlorite and the scavenging effect of SDG

The fluorescence intensity of ROS probes APF and HPF (10 μM) in PBS, pH 7.4 (DPBS: 137 mM NaCl, 2.7 mM KCl, 10 mM Na_2HPO_4 and 2 mM KH_2PO_4) was measured at excitation/emission wavelengths of 490 nm/515 nm in a Molecular Dynamics M5 fluorescence reader. Data are expressed as relative fluorescence units (RFU).

2.3. γ-Radiation-induced generation of hypochlorite and the scavenging effect of SDG

PBS, pH 7.4 (DPBS) with APF or HPF was exposed to doses of γ-radiation ranging from 2.5 to 50 Gy using a Mark 1 cesium (137Cs) irradiator (J.L. Shepherd, San Fernando, CA) at a dose rate of 1.7 Gy/min in room air (21% O_2). In addition, experiments were also

performed with various concentrations of SDG. Following radiation, the fluorescence of APF and HPF was determined. Data are expressed as relative fluorescence units (RFU).

2.4. γ-Radiation-induced generation of hypochlorite by determining taurine chloramine

Chlorination of taurine was determined using TMB assay [43]. Samples containing taurine (5.0 mM) in PBS (1×, 5× and 10×) were exposed to γ-radiation (50, 100 and 200 Gy) at 0–4 °C. After 60 min on ice, TMB reagent was added and the absorbance read in a Bio-Rad Microplate reader using 655 nm filter. A standard curve was generated using taurine chlorination in the presence of sodium hypochlorite ranging 0–40 μM. Samples were evaluated in quadruplicate and the data are expressed as taurine chloramine (absorbance) as well as ClO^- concentration (μM).

2.5. Hypochlorite-induced damage to calf thymus DNA and the effect of SDG

Calf thymus DNA (500 ng) was incubated with hypochlorite (0.1 to 0.6 mM) for 2 h at 37 °C and the reaction terminated by adding 10 mM L-methionine. The reaction was performed using 0.5 mM ClO^- and in the presence 0.5 μM SDGs, quercetin and silibinin. The selection of silibinin as a reference compound for comparing the hypochlorite scavenging ability of SDG, was not based on its structural characteristics, but based instead on its known hypochlorite scavenging action. [22]. DNA samples were subjected to agarose (1%) gel electrophoresis and analyzed as previously described [40]. The density of the high molecular weight (>6000 bps) and the low molecular weight (<6000 bps) fragments of calf thymus DNA are expressed as the percent of the total density (high molecular weight + low molecular weight DNA fragments). Densitometric analysis of high molecular weight (>6000 bps) and low molecular weight (<6000 bps) fragments of calf thymus DNA was determined by quantifying the total density of respective bands using Gel-Pro Analyzer (version 6.0; MediaCybernetics, Silver Spring, MD).

2.6. Determination of hypochlorite-induced plasmid DNA relaxation

Plasmid DNA (500 ng) in PBS (pH 7.4) was incubated with ClO^-(4.5 mM) and commercially-available SDG (25 μM) at 37 °C and the reaction terminated with 10 mM L-methionine. Samples were electrophoresed on an agarose (1%) gel and analyzed as described [40]. The density of the open-circular (OC) and the supercoiled (SC) plasmid DNA bands are expressed as the percent of the total density (open-circular + supercoiled). Densitometric analysis was performed using Gel-Pro Analyzer (version 6.0; MediaCybernetics, Silver Spring, MD).

2.7. Determination of hypochlorite-induced chlorination of 2-aminopurine (2-AP)

2-AP (10 μM) in PBS with and without commercially available SDG (20 μM) was exposed to hypochlorite (15 μM). Fluorescence spectra of 2-AP were determined using an excitation wavelength of 310 nm and the spectra recorded between 360 and 390 nm with the emission maximum at 374 nm. The percent change (calculated from untreated) in 2-AP was calculated in the presence of ClO^- as well as with SDG treatments.

2.8. Determination of γ-radiation-induced chlorination of 2-AP

2-AP (10 μM) in PBS with and without commercially available SDG (5 μM) was exposed to γ-radiation at doses 0, 25, 50 and 100 Gy. Fluorescence spectra of 2-AP were determined as described above. The fluorescence intensity was determined at 374 nm and the data are presented as the mean RFU + the standard error of the mean.

2.9. ^{1}H NMR studies

^{1}H NMR studies were performed using a Bruker DMX-360 spectrometer, working under TopSpin™ (Bruker, Germany) software, in D_2O using TSP as an internal standard. Chemical shifts are reported in ppm. The reactions were carried out in deuterated saline (0.9% NaCl in D_2O) and the spectra of the solutions were recorded before and after gamma irradiation. The control experiments without NaCl and those without dopamine and SDG were carried out under the same reaction conditions. The data were analyzed using MestReNova Lite software (Mestrelab Research, Santiago de Compostela, Spain). A typical experiment: 1 ml of 0.53 μM solution of dopamine hydrochloride or 0.265 μM solution of SDG in 0.9% NaCl in D_2O was placed in a 1.5 ml Eppendorf tube and irradiated with 100 Gy. The reaction mixture was immediately moved into a 5 mm NMR tube and the spectrum was recorded (NS = 1024).

2.10. Statistical analysis of the data

The data obtained are presented as mean values + the standard error of the mean (SEM). The data were subjected to one-way analysis of variance (ANOVA) with post-hoc comparisons using the Bonferroni/Dunn test (Statview 4.0). Differences between treatment groups were determined at alpha = 0.05, and * and # indicate statistically significant differences ($p < 0.05$).

3. Results

In the current study we investigated the ability of SDG to scavenge radiation-induced ACS, as a potential mechanism of DNA radioprotection in physiological solutions.

3.1. Cl^--containing physiological solutions scavenge $^\bullet$OH radicals generated by γ-radiation

It is commonly accepted that radiation generates extremely reactive $^\bullet$OH radicals, which cause deleterious effects in living organisms. However, this hypothesis is questionable, as the life time of $^\bullet$OH is too short and, when produced, cannot reach biomolecules such as DNA. Physiological solutions contain ~0.9% of Cl^-, which react with $^\bullet$OH. Thus, we have suggested that the damaging molecules generated by γ-radiation may potentially be ACS; among them free chlorine atoms, the primary products of the single electron transfer reactions between $^\bullet$OH and Cl^-, and HOCl, produced by disproportionation of Cl_2 in water. To demonstrate the effect of Cl^- on γ-radiation-induced generation of $^\bullet$OH, we irradiated phosphate buffer (PB), PBS and saline alone in the presence of 3′-(*p*-hydroxyphenyl) fluorescein (HPF), which is a fluorescent probe [44] selective to $^\bullet$OH. This conjugate of fluorescein and hydroquinone does not fluoresce, but can be cleaved under the action of $^\bullet$OH restoring fluorescence [41]. The results (Fig. 1) show that in the presence of Cl^- more than 90% of $^\bullet$OH are scavenged – 92% in PBS ([Cl^-] = 0.137 M) and 94% in saline ([Cl^-] =

0.154 M). This result supports our hypothesis and lead us to further investigate the role of ACS as potential damaging species produced by γ-radiation in physiological solutions.

3.2. SDG and dopamine scavenge ACS produced by γ-radiation of saline - ^{1}H NMR study

To elucidate the possible formation of active chlorine species by γ-irradiation in physiological solutions, we utilized ^{1}H NMR to study this reaction. SDG and its simplified structural analog dopamine, which both have hydroxyphenylmethyl fragments containing benzyl $ArCH_2$ protons sensitive to radical substitution (such as chlorination by chlorine atoms), were evaluated. The reaction of dopamine with hypochlorite was recently investigated by NMR and revealed chlorination of aromatic and nitrogen parts of the dopamine molecule with NaOCl solutions in the presence of small amounts HCl thus providing maximum concentration of HOCl, which chlorinated an *ortho*-position in the aromatic ring and the nitrogen atom. [42], HOCl is well known to chlorinate aromatic compounds via the mechanism of electrophilic substitution [45–48]. In our experiments for dopamine solutions we did not find changes in spectra similar to those caused by reaction with NaOCl/HOCl [42]. Instead, we found a new signal at 3.77 ppm. According to the literature, this chemical shift corresponds to the signal of methylene β-protons in a Ph(Ar)-CCl_2-CH_2-N structural fragment [49] (Fig. 2A and B). This indicates that benzylic α-hydrogens have been substituted with chlorine atoms, which occurs only by radical mechanism, i.e. active species are Cl• and/or $Cl_2^{\bullet-}$.

Chlorine atoms are a result of single electron oxidation of Cl^- by $^{\bullet}OH$. Control experiments without NaCl showed no signal at 3.77 ppm. Integration revealed that 2 ± 0.1% of dopamine was converted. We also observed new upfield signals on the right side of the aromatic peaks at 6.85, 6.93 and 6.76 ppm that corresponds to the product of dopamine chlorination (Fig. 2B), which, we suggest, belong to aromatic protons of the dichlorobenzyl fragment. Similar small right shifted signals at 6.80, 6.65 and 6.53 ppm were detected in the spectrum of SDG irradiated in saline, while absent without NaCl. This indicates that a product of SDG irradiated in saline also contains a CCl_2-group at the aromatic ring (Fig. 2C and D). At half the concentration of dopamine, integration revealed SDG conversion equal to 2 ± 0.1%, a similar level observed for dopamine. The same conversion can easily be explained by the structure of these two molecules. While SDG contains four benzylic hydrogen atoms, dopamine contains only two benzylic hydrogens. Benzylic hydrogens are exclusively sensitive to radical substitution reactions. These results indicate that primary formed ACS are radical particles such as Cl• and/or $Cl_2^{\bullet-}$. While radical substitutive chlorination of benzylic hydrogens by Cl• is well known, the same process mediated by $Cl_2^{\bullet-}$ was described only recently [50]. A possible mechanism of radical chlorination of dopamine and SDG is presented in Scheme 1 (formation of ACS is shown according to ref. [38], Scheme 1B). Knowing the concentration of starting materials (dopamine 0.53 μM and SDG 0.265 μM), sample volumes 1 ml, cross-section ~1 cm^3, and radiation dose 100 Gy, we can estimate the amount of ACS consumed. The formula for 1 Gy is:

$$\Phi \sim 6.24 \times 109 \times \frac{\ell}{Ef}$$

[51] where Φ is the fluence (photons/cm^2) of photons needed to deposit 1 Gy, ℓ is the attenuation length (g/cm^2), E is the photon energy (MeV), and f is the fraction of photon energy converted on-average to the Compton scattered electrons. In our case it is 6.24×10^9 × attenuation (~11.5 g/cm^2 for Cs in water)/(average Compton energy ~0.25 MeV for Cs-137 in water) = ~300 billion photons (3×10^{11}/cm^2); thus, for 100 Gy we get ~30 trillion or 3×10^{13} photons/cm^2. Next, after dividing by Avogadro number 6.022×10^{23}, we obtain 5×10^{-11} mol of total γ-photons. For 1 ml of dopamine (0.53 μμ) we calculated 53×10^{-11} mol. 2% yield of the reaction product corresponds to ~1×10^{-11} mol of dichloro-dopamine. Each dichloro-dopamine molecule is produced with four chlorine atoms (Scheme 1 C, C_1) or 4×10^{-11} mol ACS. Even assuming that one γ-photon can produce two hydroxyl radicals (a simplified process is shown in Scheme 1A) and each •OH produces one chlorine atom in the reaction with Cl^- (Scheme 1B), dopamine consumed ACS produced by 40% of total photons. The same values are obtained for SDG as it contains two benzyl moieties (Scheme 1C, C_2), that provide twice more efficiency at half the concentration.

In one substitution step two chlorine atoms are involved. For dichlorination of one molecule of dopamine four radical ACS are required and for chlorination of SDG in two benzyl positions eight radical ACS are required. Scheme 1D also suggests that HOCl/ClO^- are secondary ACS formed by disproportionation of Cl_2 in water. Formation of hypochlorite by γ-irradiation in the absence of radical traps (such as SDG, dopamine) was demonstrated by reaction with taurine (vide infra).

3.3. SDG scavenges hypochlorite ions

As hypochlorite is the secondary ACS formed by chlorine disproportionation (Scheme 1D) the specificity of the selected fluoroprobes was evaluated using sodium hypochlorite. Fig. 3A shows a linear increase in APF fluorescence intensity with an increase in ClO^- concentration (1–4 μM). Importantly, HPF fluorescence intensity increased only marginally, indicating that APF fluorescence is mainly ClO^--dependent. ClO^- concentrations were selected to be within this range for subsequent experiments. The ability of SDG (commercially available) to scavenge ClO^- was then evaluated. Indeed, SDG decreased ClO^- concentration-dependently (Fig. 3B). Lastly, we evaluated the ClO^- scavenging effect of synthetic SDG diastereomers SDG (*S,S*) and SDG (*R,R*). At 0.5 μM, SDG (*R,R*) and SDG (*S,S*), and SDG (com) scavenged ClO^- (Fig. 3C) with a comparable potency that was similar to silibinin, an established ClO^- scavenger.

3.4. SDG scavenges γ-radiation-induced ACS

Radiation generates ClO^- dose-dependently, as evidenced by an increase in fluorescence intensity of APF. Specifically, 50 Gy γ-radiation-induced APF and HPF (Fig. 4A) was significantly decreased by SDG in a concentration-dependent manner (Fig. 4A and B). The initial slope using an exponential decay curve of the decrease for APF fluorescence was higher compared to HPF indicating a selective scavenging effect of SDG on ClO^- (Fig. 4A). The effect of SDG on APF was significantly more pronounced as compared to HPF (Fig. 4B). SDG blunted ClO^- generation from radiation exposure (25 and 50 Gy) shown by increased APF (Fig. 4C) and HPF (Fig. 4D) fluorescence ($p < 0.05$). The ratio APF/HPF decreased by SDG indicating selective scavenging of ClO^-.

3.5. Radiation dose-dependent increase in hypochlorite as chlorination of taurine

As mentioned above, the primary ACS are radicals that can be scavenged by radical traps. In the absence of the radical traps the chlorine radicals and radical anions eventually generate Cl_2 that in water disproportionates into HOCl and HCl (Scheme 1D). To establish that radiation-induced ClO^- chlorinates -NH groups in biological molecules, we evaluated radiation-induced chlorination of taurine. The results show that in normal PBS, γ-radiation significantly increased taurine chloramine formation at 50, 100, and 200 Gy indicating that γ-radiation induces ClO^- generation which was dependent on chloride concentration (Fig. 4F and G). The results provide strong evidence that radiation induces ClO^- in a physiological solution, capable of damaging biomolecules, such a DNA and proteins.

3.6. SDG protects hypochlorite-induced damage to calf thymus and plasmid DNA

We determined whether ClO^- induces damage to genomic (Fig. 5A–D) and plasmid (Fig. 5E–F) DNA. Indeed ClO^- induces DNA fragmentation in a concentration-dependent manner (Fig. 5A and B) as determined by a significant increase in low molecular weight DNA fragments. Damage to genomic DNA exposed to 0.5 mM hypochlorite was blunted by all SDGs (commercially available or synthetic), to levels comparable to quercetin, a known antioxidant and silibinin, a ClO^- scavenger (Fig. 5C and D). Similarly, damage by ClO^- to plasmid DNA was blunted by SDG (Fig. 5E and F). Specifically, we evaluated amounts of supercoiled plasmid DNA as compared to damaged, open-circular DNA which have a different mobility pattern in agarose gel electrophoresis. The presence of SDG at (25 μM) decreased the ClO^--induced damage to plasmid DNA and preserved the DNA mostly (81.3% ± 9.4%) in the supercoiled form as compared to the open-circular form (18.6% ± 9.4%).

3.7. Protective effect of SDG on hypochlorite-induced chlorination of 2-AP

To determine whether the ClO^- damage to DNA occurs by nucleobase modification, we evaluated ClO^--induced chlorination of 2-AP, a fluorescent analog of purine. Hypochlorite, given at comparable concentrations (10 μM) to those generated by radiation exposure (Figs. 3A, 4A, and 5C) significantly ($p < 0.05$) decreased 2-AP fluorescence which was prevented by pre-treatment (60 s) with SDG (Fig. 6A and B). Most importantly, post-treatment with SDG resulted in significant recovery from hypochlorite-induced 2-AP modification if added at +15, +30, +60, +120, +180 or +300 s following the exposure to ClO^- (Fig. 6B). These results demonstrate the nucleobase protective characteristic of SDG against hypochlorite-induced modification of purine bases.

3.8. Protective effect of SDG on γ-radiation-induced chlorination of 2-AP

To determine whether radiation induces nucleobase chlorination, we used the same system as described above, namely 2-AP fluorescence (Fig. 7A). Indeed, exposure to γ-radiation resulted in a dose-dependent decrease in fluorescence intensity (an observation similar to that in presence of ClO^- in Fig. 6A) which was significantly ($p < 0.05$) prevented by SDG (Fig. 7A and B). These results demonstrate that γ-radiation induces chlorination of a nucleobase and establishes the radioprotective properties of SDG against such radiation-induced modifications of purine bases.

3.9. Proposed mechanism of SDG in preventing or mitigating nucleobase chlorination by radiation

Regarding the mechanism of recovery or prevention of N-chlorinated nucleobases, we propose either a two-electron reduction of N-Cl-molecules by sugar CHOH moieties (primary CH_2OH groups can be oxidized to –COOH group by a 4-electron transfer mechanism as shown in Scheme 2. On the other hand a one-electron reduction [52,53] of the chloramine by electron rich aromatic moieties, leading to the formation of a free N-radical [54–56], which, in turn, captures hydrogen atoms from –OH groups in phenolic SDG moieties [57], cannot be completely ruled out (not shown). Scheme 2 indicates the proposed mechanism of SDG radioprotection. We suggest that SDG molecule can scavenge all possible ACS; benzylic CH_2 groups are sensitive to radical ACS, *ortho*-aromatic positions are sites for electrophilic chlorination by HOCl, sugar secondary and primary alcohol groups can be oxidized by hypochlorite [58–62] (and N—Cl compounds [63–69]). The results of our present study provide evidence, for the first time, of a new mechanism of SDG radioprotection by scavenging ACS and protecting from radiation-induced DNA damage.

4. Discussion

The results of the present study provide strong evidence that γ-radiation produces active chlorine species in physiological solutions as demonstrated by chlorination of dopamine, SDG, and taurine. These novel findings suggest chlorine atoms and dichloro radical anions as primary damaging ACS species. Exposure to γ-radiation resulted in increased taurine chloramine formation, indicating hypochlorite as a secondary damaging ACS (see Schemes 1 and 2). We demonstrated that the γ-radiation-induced production of $^{\bullet}OH$ was drastically decreased in the presence of chloride ion in PBS as well as in saline alone. Considering the high concentration of chloride ions in physiological medium in the body, the significance of production of ACS and ACS-induced damage to cellular components including DNA would be a novel and predominant mechanism of radiation damage.

SDG, a potent antioxidant and free radical scavenger, detoxified ACS generated in physiological solutions by chemical means as well as by γ-radiation. Importantly, SDG protected DNA from ACS-induced damage and we have proposed a mechanism of SDG radioprotection (see Schemes 1 and 2) that involves scavenging ACS (both radical and hypochlorite) and regeneration of amino (–NH) groups on nucleobases from chloramines (–NCl). Additionally, exposure to γ-radiation resulted in increased chlorination of a purine base that was prevented by SDG. SDG is equally effective in protecting DNA from hypochlorite-induced damage when added prior to or post exposure, acting as both a protector and mitigator of nucleobase chlorination. Synthetic SDG (*S*,*S*) and SDG (*R*,*R*) diastereomers were equally potent in scavenging ACS and preventing ACS–induced DNA damage as compared to commercially available SDG, silibinin, and quercetin (a natural antioxidant flavonoid). Combined, these results demonstrate the protective and mitigating properties of SDG for ACS-induced modification of nucleobases. An important finding of our study is the mitigating action of SDG, i.e., the ACS-scavenging ability and DNA protective action when added several minutes (up to 5 min) post exposure. The study design is in agreement with reported studies by investigators in the field of radiation mitigation

where mitigators are given either immediately after [70] or 60 min post radiation exposure as shown by Kiss et al. [71] and Vorotnikova et al. [72].

Using a mouse model of thoracic radiation damage, our group has established the tissue radioprotective role of whole grain dietary flaxseed [73,74], a grain rich in lignan polyphenols, as well as of flaxseed lignan formulations enriched in SDG [75,76]. These studies emphasized the radioprotective and radiation mitigating properties of the lignan SDG against radiation-induced tissue damage in vivo. Extracted, purified, or synthetic flaxseed SDG is a potent antioxidant in vitro as well as in vivo [77–79]. In order to explore the therapeutic potential of SDG we have synthesized SDG by a novel chemical reaction and determined the antioxidant properties of the synthetic SDGs (*R*,*R*) and SDG (*S*,*S*) diastereomers by assessing their reducing power, metal chelating potential, and free radical scavenging activity for $^{\bullet}$OH, peroxyl and DPPH radicals [39]. We also demonstrated the radioprotective characteristics of the synthetic SDGs (*R*,*R*) and SDG (*S*,*S*) diastereomers by assessing their potential for preventing γ-radiation-induced damage to plasmid DNA (pBR322) and calf thymus DNA [40].

In a separate study, we showed that the maximum radioprotection of genomic DNA by SDG was achieved at approximately 5.0 μM concentration, which is below the EC_{50} values for their free radical scavenging and antioxidant effects, typically in the range of 130–200 μM [39,77]. It is interesting to note that the maximum effectiveness of SDG in scavenging radiation-induced ACS, as determined by the present study, falls within the 0.5 to 5 μM range. This suggests that the known DNA-protective effects of SDG [40] are due in part to scavenging of damaging ACS. The results showing the protective effect of SDG on ACS-induced modification of 2-AP indicate that SDG protects DNA by preventing ACS-induced damage to nucleobases. To further elucidate the DNA protective properties of SDG, we are currently pursuing the subcellular localization of SDG in separate studies. Specifically, using cell fractionation and analytical methodologies such as LC/MS/MS, we aim to determine the intracellular fate, and kinetics of metabolic breakdown of SDG. The findings of our studies provide robust evidence of the role of harmful active chlorine species generated during radiation exposure of physiological solutions and more importantly support a novel mechanism of DNA radioprotective action of SDG. However, one should be cautioned when extrapolating to intact animals and humans as this was validated in a model system, an artificial system that is associated with certain limitations. Such are the lack of an intact cell and tissue defense system which is recruited to detoxify such harmful intermediates in an in vivo situation. Nevertheless, the findings of our study are novel and valuable in that they identify active chlorine species as significant contributors to radiation damage of macromolecules, in addition to the known reactive oxygen species.

HOCl is produced by myeloperoxidase within activated neutrophils using hydrogen peroxide generated by NADPH oxidase and chloride ions as substrates [80,81]. HOCl can chlorinate and oxidize nucleobases, resulting in potential genotoxicity. Such chlorinated nucleosides have been identified and linked to inflammation and cancer [82]. Modeling of radiation-induced DNA damage and cell death often utilizes high radiation doses [83,84].The highest dose used in our study (200 Gy) is above the clinical range and was used to ensure hypochlorite generation and DNA damage; however, we have shown that DNA damaging

hypochlorite levels are also generated with lower radiation doses such as 50 Gy that are close to what is used clinically. Specifically, 34 Gy single fractions are now routinely used in stereotactic radiotherapy to treat cancer [85].

There could be several potential mechanisms by which SDG protects DNA from radiation-induced damage: 1) by scavenging ACS (both radical species and hypochlorite ions) that cause chlorination and oxidation of nucleobases; 2) by scavenging $^{\bullet}OH$ free radicals that produce ACS when reacting with chloride ions; 3) by associating with DNA base pairs similar to flavonoids such as lutiolin, kempferol and quercetin [86–88]; 4) by blocking abstraction of protons or addition of $^{\bullet}OH$ on the purine and pyrimidine bases especially at C5, C6 and C8, and at the deoxyribose sites, which have been proposed for protection from free radical-induced DNA damage [16,26,27,89]; 5) lastly, by reduction of chloroamines formed, thus, regenerating internal and external amino groups in nucleic acids. Therefore, SDG as a scavenger of ACS, as well as being an antioxidant, free radical scavenger and protector of nucleobases from ACS-induced chlorination, can function as a potential DNA radioprotector and mitigator. The radiation doses selected for the studies described here, ranging mostly around 50 Gy, are clinically relevant and based on doses used for radiotherapy patients [90].

Hypochlorite exists in solution as a mixture of hypochlorite anion (ClO^{-}), hypochlorous acid (HOCl) and free chlorine (Cl_2) in pH-dependent amounts [91]. At physiological pH, ClO^{-} and HOCl are the predominant molecules. Unlike strong, single-electron oxidants such as $^{\bullet}OH$, hypochlorite is a two-electron oxidant, less reactive and more selective than $^{\bullet}OH$. Hypochloric acid can chlorinate electron-rich aromatic rings and NH-compounds. Hypochlorite oxidizes primary and secondary alcohols, and phenols. The first step of the above reactions is chlorination followed by hydrolysis/HCl elimination [91,92]. It is important to note that SDG contains all the reaction sites stated above (except amino groups), making the SDG molecule a potent hypochlorite scavenger. Additionally, the benzylic methylene groups of SDG, reacts with chlorine atoms, dichloro radical anions; the intermediate benzylic radicals reacts with chlorine molecules (Scheme 1). In Scheme 2, we propose a novel mechanism of DNA protection by SDG using a reduction of a nucleobase.

In summary, we have demonstrated that SDG effectively scavenges ACS, both primary radical species Cl• and $Cl_2^{\bullet -}$ and secondary hypochlorite ions, and prevents radiation-induced DNA damage. Since hypochlorite ions are known to modify DNA bases by chlorination/oxidation, resulting in DNA damage, our findings may aid in the development of SDG as a potential radioprotector of normal tissue damage associated with radiotherapy for cancer treatment or as a mitigator of accidental exposure to radiation.

Acknowledgments

Funding

This work was funded in part by: NIH-R01 CA133470 (MCS), NIH-1R21NS087406-01 (MCS), NIH-R03 CA180548 (MCS), 1P42ES023720-01 (MCS) and by pilot project support from 1P30 ES013508-02 awarded to MCS (its contents are solely the responsibility of the authors and do not necessarily represent the official views of the NIEHS, NIH). Supported in part (AVP) by Grant #IRG-78-002-31 is from the American Cancer Society. The authors wish to thank Dr. Nadia Anikeeva for useful suggestions and Dr. E.J. Delikatny for critical reading of the manuscript and discussion.

Abbreviations

2-AP	2-aminopurine
ACS	active chlorine species
ANOVA	analysis of variance
APF	3′-(*p*-aminophenyl) fluorescein
Cl•	chlorine atom
Cl^-	chloride anion
Cl_2	chlorine
$Cl_2^{\bullet -}$	dichloro radical anion
ClO^-	hypochlorite ion
H_2O_2	hydrogen peroxide
HOCl	hypochlorous acid
HPF	3′-(*p*-hydroxyphenyl) fluorescein
$^{\bullet}OH$	hydroxyl radical
OC	open-circular DNA
PBS	phosphate-buffered saline
RFU	relative fluorescence units
ROS	reactive oxygen species
SC	supercoiled DNA
SDG	secoisolariciresinol diglucoside
SEM	standard error of the mean

References

1. Park H, Vecitis CD, Hoffmann MR. Electrochemical water splitting coupled with organic compound oxidation: the role of active chlorine species. J Phys Chem C. 2009; 113:7935–7945.
2. Jang J, Jang M, Mui W, Delcomyn CA, Henley MV, Hearn JD. Formation of active chlorine oxidants in saline-oxone aerosol. Aerosol Sci Technol. 2010; 44:1018–1026.
3. Degaki AH, Pereira GF, Rocha-Filho RC, Bocchi N, Biaggio SR. Effect of specific active chlorine species and temperature on the electrochemical degradation of the reactive blue 19 dye using a boron-doped diamond or DSA anode in a flow reactor. Electrocatalysis. 2014; 5:8–15.
4. Brito, CdN, de Araujo, DM., Martinez-Huitle, CA., Rodrigo, MA. Understanding active chlorine species production using boron doped diamond films with lower and higher sp3/sp2 ratio. Electrochem Commun. 2015; 55:34–38.

5. Albert CJ, Crowley JR, Hsu FF, Thukkani AK, Ford DA. Reactive chlorinating species produced by myeloperoxidase target the vinyl ether bond of plasmalogens. Identification of 2-chlorohexadecanal. J Biol Chem. 2001; 276:23733–23741. [PubMed: 11301330]
6. de Moura DC, de Araujo CKC, Zanta CLPS, Salazar R, Martinez-Huitle CA. Active chlorine species electrogenerated on Ti/Ru0·3Ti0.7O_2 surface: electrochemical behavior, concentration determination and their application. J Electroanal Chem. 2014; 731:145–152.
7. Pudtikajorn K, Shin I-s, Jeong W-S, Chung D. Kinetic modeling of active chlorine generation by low-amperage pulsating direct current in a circulating brine solution. J Food Eng. 2009; 92:461–466.
8. Jeitner, T., Lawrence, D. Pulmonary Autoimmunity and Inflammation. In: Cohen, MD.Zelikoff, JT., Schlesinger, RB., editors. Pulmonary Immunotoxicology. Kluwer Academic Publishers; New York: 2000. p. 153-179.
9. Spessotto P, Dri P, Bulla R, Zabucchi G, Patriarca P. Human eosinophil peroxidase enhances tumor necrosis factor and hydrogen peroxide release by human monocyte-derived macrophages. Eur J Immunol. 1995; 25:1366–1373. [PubMed: 7774640]
10. Wang J, Slungaard A. Role of eosinophil peroxidase in host defense and disease pathology. Arch Biochem Biophys. 2006; 445:256–260. [PubMed: 16297853]
11. Bernofsky C. Nucleotide chloramines and neutrophil-mediated cytotoxicity. FASEB J. 1991; 5:295–300. [PubMed: 1848195]
12. Bernofsky C, Bandara BMR, Hinojosa O, Strauss SL. Hypochlorite-modified adenine nucleotides: structure, spin-trapping, and formation by activated guinea pig polymorphonuclear leukocytes. Free Radic Res Commun. 1990; 9:303–315. [PubMed: 2167269]
13. Henderson JP, Byun J, Heinecke JW. Chlorination of nucleobases, RNA and DNA by myeloperoxidase: a pathway for cytotoxicity and mutagenesis by activated phagocytes. Redox Rep. 1999; 4:319–320. [PubMed: 10772075]
14. Hawkins CL, Davies MJ. Hypochlorite-induced damage to DNA, RNA, and polynucleotides: formation of chloramines and nitrogen-centered radicals. Chem Res Toxicol. 2002; 15:83–92. [PubMed: 11800600]
15. Hawkins CL, Pattison DI, Davies MJ. Hypochlorite-induced oxidation of amino acids, peptides and proteins. Amino Acids. 2003; 25:259–274. [PubMed: 14661089]
16. Cadet J, Wagner JR. DNA base damage by reactive oxygen species, oxidizing agents, and UV radiation. Cold Spring Harb Perspect Biol. 2013; 5 (A012559/012551-A012559/012518).
17. Jeitner TM, Xu H, Gibson GE. Inhibition of the α-ketoglutarate dehydrogenase complex by the myeloperoxidase products, hypochlorous acid and mono-*N*-chloramine. J Neurochem. 2005; 92:302–310. [PubMed: 15663478]
18. Masuda M, Suzuki T, Friesen MD, Ravanat JL, Cadet J, Pignatelli B, Nishino H, Ohshima H. Chlorination of guanosine and other nucleosides by hypochlorous acid and myeloperoxidase of activated human neutrophils: catalysis by nicotine and trimethylamine. J Biol Chem. 2001; 276:40486–40496. [PubMed: 11533049]
19. Badouard C, Masuda M, Nishino H, Cadet J, Favier A, Ravanat JL. Detection of chlorinated DNA and RNA nucleosides by HPLC coupled to tandem mass spectrometry as potential biomarkers of inflammation. J Chromatogr B Anal Technol Biomed Life Sci. 2005; 827:26–31.
20. Prutz WA. Hypochlorous acid interactions with thiols, nucleotides, DNA, and other biological substrates. Arch Biochem Biophys. 1996; 332:110–120. [PubMed: 8806715]
21. Prutz WA. Interactions of hypochlorous acid with pyrimidine nucleotides, and secondary reactions of chlorinated pyrimidines with GSH, NADH, and other substrates. Arch Biochem Biophys. 1998; 349:183–191. [PubMed: 9439597]
22. Nakano T, Masuda M, Suzuki T, Ohshima H. Inhibition by polyphenolic phytochemicals and sulfurous compounds of the formation of 8-chloroguanosine mediated by hypochlorous acid, human myeloperoxidase, and activated human neutrophils. Biosci Biotechnol Biochem. 2012; 76:2208–2213. [PubMed: 23221717]
23. Lahtz C, Bates SE, Jiang Y, Li AX, Wu X, Hahn MA, Pfeifer GP. Gamma irradiation does not induce detectable changes in DNA methylation directly following exposure of human cells. PLoS One. 2012; 7:e44858. [PubMed: 23024770]

24. Feldberg RS, Carew JA. Water radiolysis products and nucleotide damage in γ-irradiated DNA. Int J Radiat Biol Relat Stud Phys Chem Med. 1981; 40:11–17. [PubMed: 6266972]
25. Kuipers GK, Lafleur MVM. Characterization of DNA damage induced by gamma-radiation-derived water radicals, using DNA repair enzymes. Int J Radiat Biol. 1998; 74:511–519. [PubMed: 9798962]
26. Cadet J, Douki T, Ravanat JL. Oxidatively generated base damage to cellular DNA. Free Radic Biol Med. 2010; 49:9–21. [PubMed: 20363317]
27. Spotheim-Maurizot M, Davidkova M. Radiation damage to DNA in DNA-protein complexes. Mutat Res Fundam Mol Mech Mutagen. 2011; 711:41–48.
28. Saran M, Bertram H, Bors W, Czapski G. On the cytotoxicity of irradiated media. To what extent are stable products of radical chain reactions in physiological saline responsible for cell death? Int J Radiat Biol. 1993; 64:311–318. [PubMed: 8105009]
29. Saran M, Bors W. Radiation chemistry of physiological saline reinvestigated: evidence that chloride-derived intermediates play a key role in cytotoxicity. Radiat Res. 1997; 147:70–77. [PubMed: 8989372]
30. Krokosz A, Komorowska MA, Szweda-Lewandowska Z. Radiation damage to human erythrocytes. Relative contribution of hydroxyl and chloride radicals in N_2O-saturated buffers. Radiat Phys Chem. 2008; 77:775–780.
31. Kudryasheva, NS., Rozhko, TV. Effect of low-dose ionizing radiation on luminous marine bacteria: radiation hormesis and toxicity. J Environ Radioact. 2015. http://dx.doi.org/10.1016/j.jenvrad.2015.1001.1012/
32. Cachet H, Festy D, Folcher G, Mazeas F, Tribollet B. Electrochemical protection of windows immersed in seawater against biofouling. Mater Technol. 2002; 90:37–42.
33. Cardenas A, Zayas T, Morales U, Salgado L. Electrochemical oxidation of wastewaters from the instant coffee industry using a dimensionally stable RuIrCoOx anode. ECS Trans. 2009; 20:291–299.
34. Kim J, Choi WJK, Choi J, Hoffmann MR, Park H. Electrolysis of urea and urine for solar hydrogen. Catal Today. 2013; 199:2–7.
35. Shaarawy HH, Saied M. Production of sodium hypochlorite or mixed oxidant using rhodium/rhodium oxide mixed modified electrode. Aust J Basic Appl Sci. 2012; 6:204–215.
36. Shih YJ, Chen KH, Huang YH. Mineralization of organic acids by the photo-electrochemical process in the presence of chloride ions. J Taiwan Inst Chem Eng. 2014; 45:962–966.
37. Wang B, Liang B, Li G, Feng Y, Hu C. Electro-catalytic oxidative degradation of aniline with RuOx-PdO/Ti electrode. Guijinshu. 2005; 26:25–31.
38. Sires I, Garrido JA, Brillas E. Performance of the electro-oxidation and electro-Fenton processes with a BDD anode for the treatment of low contents of pharmaceuticals in a real water matrix. Dianhuaxue. 2013; 19:300–312.
39. Mishra OP, Simmons N, Tyagi S, Pietrofesa R, Shuvaev VV, Valiulin RA, Heretsch P, Nicolaou KC, Christofidou-Solomidou M. Synthesis and antioxidant evaluation of (*S,S*)- and (*R,R*)-secoisolariciresinol diglucosides (SDGs). Bioorg Med Chem Lett. 2013; 23:5325–5328. [PubMed: 23978651]
40. Mishra OP, Pietrofesa R, Christofidou-Solomidou M. Novel synthetic (*S,S*) and (*R,R*)-secoisolariciresinol diglucosides (SDGs) protect naked plasmid and genomic DNA from gamma radiation damage. Radiat Res. 2014; 182:102–110. [PubMed: 24945894]
41. Setsukinai, K-i, Urano, Y., Kakinuma, K., Majima, HJ., Nagano, T. Development of novel fluorescence probes that can reliably detect reactive oxygen species and distinguish specific species. J Biol Chem. 2003; 278:3170–3175. [PubMed: 12419811]
42. Jeitner TM, Kalogiannis M, Patrick PA, Gomolin I, Palaia T, Ragolia L, Brand D, Delikatny EJ. Inflaming the diseased brain: a role for tainted melanins. Biochim Biophys Acta Mol basis Dis. 2015; 1852:937–950.
43. Dypbukt JM, Bishop C, Brooks WM, Thong B, Eriksson H, Kettle AJ. A sensitive and selective assay for chloramine production by myeloperoxidase. Free Radic Biol Med. 2005; 39:1468–1477. [PubMed: 16274882]

44. Popov AV, Mawn TM, Kim S, Zheng G, Delikatny EJ. Design and synthesis of phospholipase C and A2-activatable near-infrared fluorescent smart probes. Bioconjug Chem. 2010; 21:1724–1727. [PubMed: 20882956]
45. Carlson RM, Carlson RE, Kopperman HL, Caple R. Facile incorporation of chlorine into aromatic systems during aqueous chlorination processes. Environ Sci Technol. 1975; 9:674–675.
46. Deborde M, von Gunten U. Reactions of chlorine with inorganic and organic compounds during water treatment - kinetics and mechanisms: a critical review. Water Res. 2008; 42:13–51. [PubMed: 17915284]
47. Gowda BT, Mary MC. Kinetics and mechanism of chlorination of phenol and substituted phenols by sodium hypochlorite in aqueous alkaline medium. Indian J Chem, Sect A: Inorg, Bioinorg, Phys, Theor Anal Chem. 2001; 40A:1196–1202.
48. Hopkins CY, Chisholm MJ. Chlorination by aqueous sodium hypochlorite. Can J Res Sect B. 1946; 24B:208–210.
49. Rozentsveig GN, Popov AV, Rozentsveig IB, Levkovskaya GG. Reduction of *N*-(polychloroethylidene)- and N-(1-hydroxypolychloroethyl) arenesulfonamides with adamantane in the presence of superacids. Russ J Org Chem. 2011; 47:520–522.
50. Martire DO, Rosso JA, Bertolotti S, Le Roux GC, Braun AM, Gonzalez MC. Kinetic study of the reactions of chlorine atoms and $Cl_2^{\bullet-}$ radical anions in aqueous solutions. II. Toluene, benzoic acid, and chlorobenzene. J Phys Chem A. 2001; 105:5385–5392.
51. Olive KA, Agashe K, Arnsler C, Antonei M, Arguin JF, Asner DM, Baer H, Band HR, Barnett RM, Basaglia T, Bauer CW, Beatty JJ, Beousov VI, Beringer J, Bernardi G, Bethke S, Bichsel H, Biebel O, Blucher E, Blusk S, Brooijmans G, Buchmueller O, Burkert V, Bychkov MA, Cahn RN, Carena M, Ceccucci A, Cerri A, Chakraborty D, Chen MC, Chivukula RS, Copic K, Cowan G, Dahl O, D'Ambrosio G, Damour T, de Forian D, de Gouvea A, DeGrand T, de Jong P, Dissertori G, Dobrescu BA, Doser M, Drees M, Dreiner HK, Edwards DA, Eidelman S, Erler J, Ezhea VV, Fetscher W, Fields BD, Foster B, Freitas A, Gaisser TK, Gallagher H, Garren L, Gerber HJ, Gerbier G, Gershon T, Gherghetta T, Gowala S, Goodman M, Grab C, Gritsan AV, Grojean C, Groom DE, Grunewald M, Gurtu A, Gutsche T, Haber HE, Hagiwara K, Hanhart C, Hashimoto S, Hayato Y, Hayes KG, Heffner M, Hetsley B, Hernandez-Rey JJ, Hikasa K, Hocker A, Holder J, Holtkamp A, Huston J, Jackson JD, Johnson KF, Junk T, Kado M, Karlen D, Katz UF, Klein SR, Klempt E, Kowalewski RV, Krauss F, Kreps M, Krusche B, Kuyanov YV, Kwon Y, Lahav O, Laiho J, Langacker P, Liddle A, Ligeti Z, Lin CJ, Liss TM, Littenberg L, Lugovsky KS, Lugovsky SB, Matolni F, Mannel T, Manohar AV, Marciano WJ, Martin AD, Masoni A, Matthews J, Milstead D, Molaro P, Moenig K, Moortgat F, Mortonson MJ, Murayama H, Nakamura K, Narain M, Nason P, Navas S, Neubert M, Nevski P, Nir Y, Pape L, Parsons J, Patrignani C, Peacock JA, Pennington M, Petcov ST, Piepke A, Pomarol A, Quadt A, Raby S, Rademacker J, Raffelt G, Ratcliff BN, Richardson P, Ringwald A, Roesler S, Rolli S, Romaniouk A, Rosenberg LJ, Rosner JL, Rybka G, Sachrajda CT, Sakai Y, Salam GP, Sarkar S, Sauli F, Schneider O, Schoberg K, Scott D, Sharma V, Sharpe SR, Silari M, Sjoestrand T, Skands P, Smith JG, Smoot GF, Spanier S, Spieler H, Spiering C, Stahl A, Stanev T, Stone SL, Sumiyoshi T, Syphers MJ, Takahashi F, Tanabashi M, Terning J, Tiator L, Titov M, Tkachenko NP, Tornqvist NA, Tovey D, Valencia G, Venanzoni G, Vincter MG, Vogel P, Vogt A, Wakley SP, Wakowiak W, Walter CW, Ward DR, Weiglein G, Weinberg DH, Weinberg EJ, White M, Wiencke LR, Wohl CG, Wofenstein L, Womersley J, Woody CL, Workman RL, Yamamoto A, Yao WM, Zeller GP, Zenin OV, Zhang J, Zhu RY, Zimmermann F, Zyla PA. Review of particle physics. Chin Phys C. 2014; 38:090001/090001–090001/091676.
52. Percec V, Popov AV. Functionalization of the active chain ends of poly(vinyl chloride) obtained by single-electron-transfer/degenerative-chain-transfer mediated living radical polymerization: synthesis of telechelic α,ω-di(hydroxy)poly(vinyl chloride). J Polym Sci A Polym Chem. 2005; 43:1255–1260.
53. Percec V, Popov AV, Ramirez-Castillo E. Single-electron-transfer/degenerative-chain-transfer mediated living radical polymerization of vinyl chloride catalyzed by thiourea dioxide/octyl viologen in water/tetrahydrofuran at 25 °C. J Polym Sci A Polym Chem. 2005; 43:287–295.
54. Hawkins CL, Davies MJ. Hypochlorite-induced damage to proteins: formation of nitrogen-centered radicals from lysine residues and their role in protein fragmentation. Biochem J. 1998; 332:617–625. [PubMed: 9620862]

55. Hawkins CL, Davies MJ. Hypochlorite-induced damage to nucleosides: formation of chloramines and nitrogen-centered radicals. Chem Res Toxicol. 2001; 14:1071–1081. [PubMed: 11511181]
56. Hawkins CL, Davies MJ. Hypochlorite-induced damage to red blood cells. Evidence for the formation of nitrogen-centered radicals. Redox Rep. 2000; 5:57–59. [PubMed: 10905549]
57. Hosseinian FS, Muir AD, Westcott ND, Krol ES. AAPH-mediated antioxidant reactions of secoisolariciresinol and SDG. Org Biomol Chem. 2007; 5:644–654. [PubMed: 17285173]
58. Battistelli CL, De Castro C, Iadonisi A, Lanzetta R, Mangoni L, Parrilli M. Synthesis and NMR characterization of methyl mono- and di-*O*-α-*L*-rhamnopyranosyl-α-*D*-glucopyranosiduronic acids. J Carbohydr Chem. 1999; 18:69–86.
59. Bonfatti F, Ferro S, Lavezzo F, Malacarne M, Lodi G, De Battisti A. Electrochemical incineration of glucose as a model organic substrate II. Role of active chlorine mediation. J Electrochem Soc. 2000; 147:592–596.
60. De Lederkremer RM, Marino C. Acids and other products of oxidation of sugars. Adv Carbohydr Chem Biochem. 2003; 58:199–306. [PubMed: 14719360]
61. Grigor TT, Tumanova TA, Mishchenko KP, Salanki L. Reaction of glucose with sodium hypochlorite in aqueous solution as model for pulp bleaching. Zh Prikl Khim. 1967; 40:2039–2044.
62. Whistler RL, Schweiger R. Preparation of D-arabinose from D-glucose with hypochlorite. J Am Chem Soc. 1959; 81:5190–5192.
63. Rangappa KS, Raghavendra MP, Mahadevappa DS, Channegowda D. Sodium *N*-chlorobenzenesulfonamide as a selective oxidant for Hexosamines in alkaline medium: a kinetic and mechanistic study. J Org Chem. 1998; 63:531–536. [PubMed: 11672041]
64. Rangappa KS, Manjunathaswamy H, Raghavendra MP, Gowda DC. Oxidation of threose-series pentoses and hexoses by sodium *N*-chloro-*p*-toluenesulfonamide. Carbohydr Res. 1998; 307:253–262.
65. Rangappa KS, Raghavendra MP, Mahadevappa DS, Gowda DC. Kinetics and mechanism of oxidation of *erythro*-series pentoses and hexoses by *N*-chloro-*p*-toluenesulfonamide. Carbohydr Res. 1998; 306:57–67. [PubMed: 9691439]
66. Raghavendra MP, Rangappa KS, Mahadevappa DS, Gowda DC. Oxidation of erythrose series sugars by sodium *N*-chlorobenzenesulfonamide in alkaline medium: a kinetic study. Indian J Chem, Sect B: Org Chem Incl Med Chem. 1998; 37B:783–792.
67. Dhoke S, Shrivastava RK. Studies on kinetics and mechanism of micellar catalyzed oxidation of pentose sugar by chloramine -T. J Ultra Chem. 2011; 7:134–138.
68. Jain S, Bakhru M, Nagwanshi R. A kinetic study of photochemical oxidation of sucrose by chloramine-T in acidic medium. J Indian Chem Soc. 2011; 88:963–967.
69. Wadhwani M, Jain S. Photochemical oxidation of some carbohydrates by chloramine-T in acidic medium. A kinetic study. Oxid Commun. 2013; 36:852–860.
70. Epperly MW, Franicola D, Shields D, Rwigema JC, Stone B, Zhang X, McBride W, Georges G, Wipf P, Greenberger JS. Screening of antimicrobial agents for in vitro radiation protection and mitigation capacity, including those used in supportive care regimens for bone marrow transplant recipients. In vivo. 2010; 24:9–19. [PubMed: 20133970]
71. Kiss GN, Lee SC, Fells JI, Liu J, Valentine WJ, Fujiwara Y, Thompson KE, Yates CR, Sumegi B, Tigyi G. Mitigation of radiation injury by selective stimulation of the LPA(2) receptor. Biochim Biophys Acta. 2013; 1831:117–125. [PubMed: 23127512]
72. Vorotnikova E, Rosenthal RA, Tries M, Doctrow SR, Braunhut SJ. Novel synthetic SOD/catalase mimetics can mitigate capillary endothelial cell apoptosis caused by ionizing radiation. Radiat Res. 2010; 173:748–759. [PubMed: 20518654]
73. Lee JC, Krochak R, Blouin A, Kanterakis S, Chatterjee S, Arguiri E, Vachani A, Solomides CC, Cengel KA, Christofidou-Solomidou M. Dietary flaxseed prevents radiation-induced oxidative lung damage, inflammation and fibrosis in a mouse model of thoracic radiation injury. Cancer Biol Ther. 2009; 8:47–53. [PubMed: 18981722]
74. Christofidou-Solomidou M, Tyagi S, Tan KS, Hagan S, Pietrofesa R, Dukes F, Arguiri E, Heitjan DF, Solomides CC, Cengel KA. Dietary flaxseed administered post thoracic radiation treatment

improves survival and mitigates radiation-induced pneumonopathy in mice. BMC Cancer. 2011; 11:269. [PubMed: 21702963]

75. Christofidou-Solomidou M, Tyagi S, Pietrofesa R, Dukes F, Arguiri E, Turowski J, Grieshaber PA, Solomides CC, Cengel KA. Radioprotective role in lung of the flaxseed lignan complex enriched in the phenolic secoisolariciresinol diglucoside (SDG). Radiat Res. 2012; 178:568–580. [PubMed: 23106213]
76. Pietrofesa R, Turowski J, Tyagi S, Dukes F, Arguiri E, Busch TM, Gallagher-Colombo SM, Solomides CC, Cengel KA, Christofidou-Solomidou M. Radiation mitigating properties of the lignan component in flaxseed. BMC Cancer. 2013; 13:179. [PubMed: 23557217]
77. Moree SS, Khanum Sa, Rajesha J. Secoisolariciresinol diglucoside - a phytoestrogen nutraceutical of flaxseed: synthesis and evaluation of antioxidant potency. Free Radicals Antioxid. 2011; 1:31–38.
78. Hu C, Yuan YV, Kitts DD. Antioxidant activities of the flaxseed lignan secoisolariciresinol diglucoside, its aglycone secoisolariciresinol and the mammalian lignans enterodiol and enterolactone in vitro. Food Chem Toxicol. 2007; 45:2219–2227. [PubMed: 17624649]
79. Moree SS, Rajesha J. Investigation of in vitro and in vivo antioxidant potential of secoisolariciresinol diglucoside. Mol Cell Biochem. 2013; 373:179–187. [PubMed: 23108790]
80. Andreyev AY, Kushnareva YE, Starkov AA. Mitochondrial metabolism of reactive oxygen species. Biochem Mosc. 2005; 70:200–214.
81. Kushnareva Y, Murphy AN, Andreyev A. Complex I-mediated reactive oxygen species generation: modulation by cytochrome *c* and NAD(P) + oxidation-reduction state. Biochem J. 2002; 368:545–553. [PubMed: 12180906]
82. Hawkins, CL., Pattison, DI., Whiteman, M., Davies, MJ. Chlorination and Nitration of DNA and Nucleic Acid Components. In: Cooke, MDEMS., editor. Oxidative Damage to Nucleic Acids. Springer; New York: 2007. p. 14-39.
83. Shuryak I, Carlson DJ, Brown JM, Brenner DJ. High-dose and fractionation effects in stereotactic radiation therapy: analysis of tumor control data from 2965 patients. Radiother Oncol. 2015; 115:327–334. [PubMed: 26058991]
84. Gameiro SR, Jammeh ML, Wattenberg MM, Tsang KY, Ferrone S, Hodge JW. Radiation-induced immunogenic modulation of tumor enhances antigen processing and calreticulin exposure, resulting in enhanced T-cell killing. Oncotarget. 2014; 5:403–416. [PubMed: 24480782]
85. Videtic GM, Hu C, Singh AK, Chang JY, Parker W, Olivier KR, Schild SE, Komaki R, Urbanic JJ, Choy H. A randomized phase 2 study comparing 2 stereotactic body radiation therapy schedules for medically inoperable patients with stage I peripheral non-small cell lung cancer: NRG oncology RTOG 0915 (NCCTG N0927). Int J Radiat Oncol Biol Phys. 2015; 93:757–764. [PubMed: 26530743]
86. Rusak G, Piantanida I, Masic L, Kapuralin K, Durgo K, Kopjar N. Spectrophotometric analysis of flavonoid-DNA interactions and DNA damaging/protecting and cytotoxic potential of flavonoids in human peripheral blood lymphocytes. Chem Biol Interact. 2010; 188:181–189. [PubMed: 20637747]
87. Zhang S, Ling B, Qu F, Sun X. Investigation on the interaction between luteolin and calf thymus DNA by spectroscopic techniques. Spectrochim Acta A. 2012; 97:521–525.
88. Marinic M, Piantanida I, Rusak G, Zinic M. Interactions of quercetin and its lanthane complex with double stranded DNA/RNA and single stranded RNA: spectrophotometric sensing of poly G. J Inorg Biochem. 2006; 100:288–298. [PubMed: 16386796]
89. Kumar A, Pottiboyina V, Sevilla MD. Hydroxyl radical (OH •) reaction with guanine in an aqueous environment: a DFT study. J Phys Chem B. 2011; 115:15129–15137. [PubMed: 22050033]
90. Chang JY, Kestin LL, Barriger RB, Chetty IJ, Ginsburg ME, Kumar S, Loo BW Jr, Movsas B, Rimner A, Rosenzweig KE, Stinchcombe TE, Videtic GM, Willers H. ACR Appropriateness Criteria (R) nonsurgical treatment for locally advanced non-small-cell lung cancer: good performance status/definitive intent. Oncology. 2014; 28:706–710. (712, 714 passim). [PubMed: 25140629]
91. Galvin, JM., Jacobsen, EN., Palucki, M. S. Hypochlorite, *e*-EROS Encyclopedia of Reagents for Organic Synthesis. John Wiley & Sons, Ltd; 2013. (pp. No pp. given)

92. Veisi H. Sodium hypochlorite (NaOCl). Synlett. 2007:2607–2608.

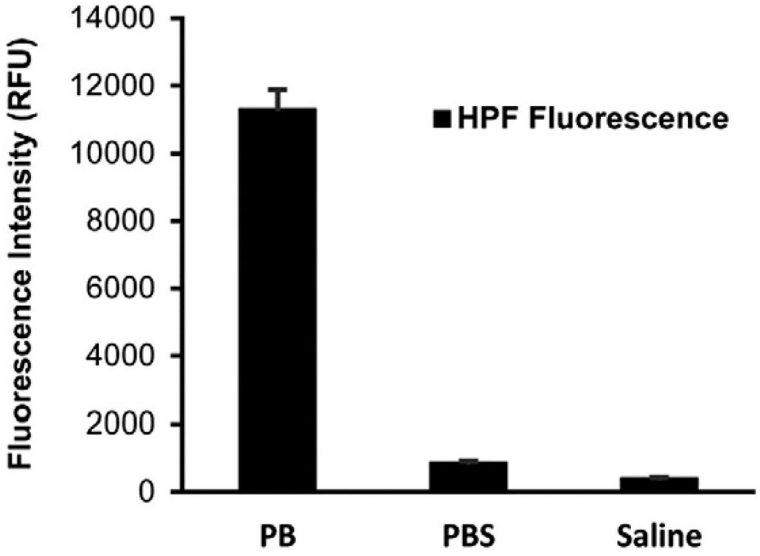

Fig. 1.

Effect of chloride-ions on radiation-induced generation of OH Radicals. Sodium phosphate buffer (pH 7.4) 50 mM, PBS (0.9%) and saline (0.9%) containing HPF probe (10 μM) were exposed to 50 Gy gamma radiation. The fluorescence intensity for HPF was measured at an excitation wavelength of 490 nm and an emission wavelength of 515 nm. The increase in fluorescence intensity of HPF was determined and the data are expressed as the mean relative fluorescence units (RFU) + SEM.

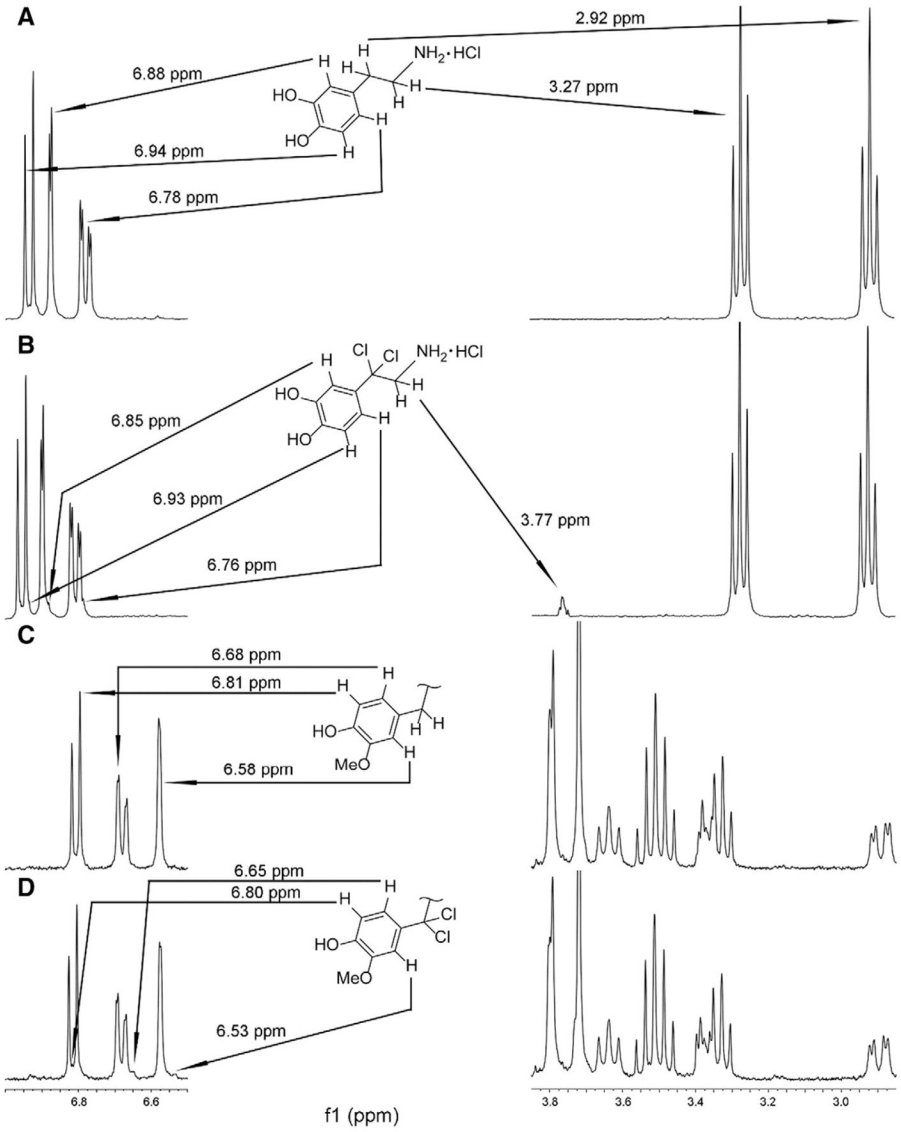

Fig. 2.

^{1}H NMR spectra of dopamine and SDG in D_2O-NaCl 0.154 M before and after γ-radiation (100 Gy). Panel 2A shows ^{1}H NMR spectrum for the solution containing dopamine and NaCl (0.154 M) in D_2O. Chemical shift values corresponding to initial and altered resonances are shown. The arrows indicate protons, their resonance positions and their chemical shifts in the structure of dopamine. Panel 2B shows ^{1}H NMR spectrum of the reaction mixture solution of dopamine and NaCl (0.154 M) in D_2O after γ-radiation (100 Gy); the arrows connect new signals and corresponding protons of the reaction product. Panel 2C represents resonances of aromatic protons of SDG as well as a fragment of the spectrum 3.85–2.85 ppm. Panel 2C also contains a benzylic structural fragment of SDG. The arrows connect aromatic SDG protons and their resonances. Panel 2D shows ^{1}H NMR spectrum of the reaction mixture solution of SDG and NaCl (0.154 M) in D_2O after γ-radiation (100 Gy). The arrows connect new signals and corresponding protons of the reaction product.

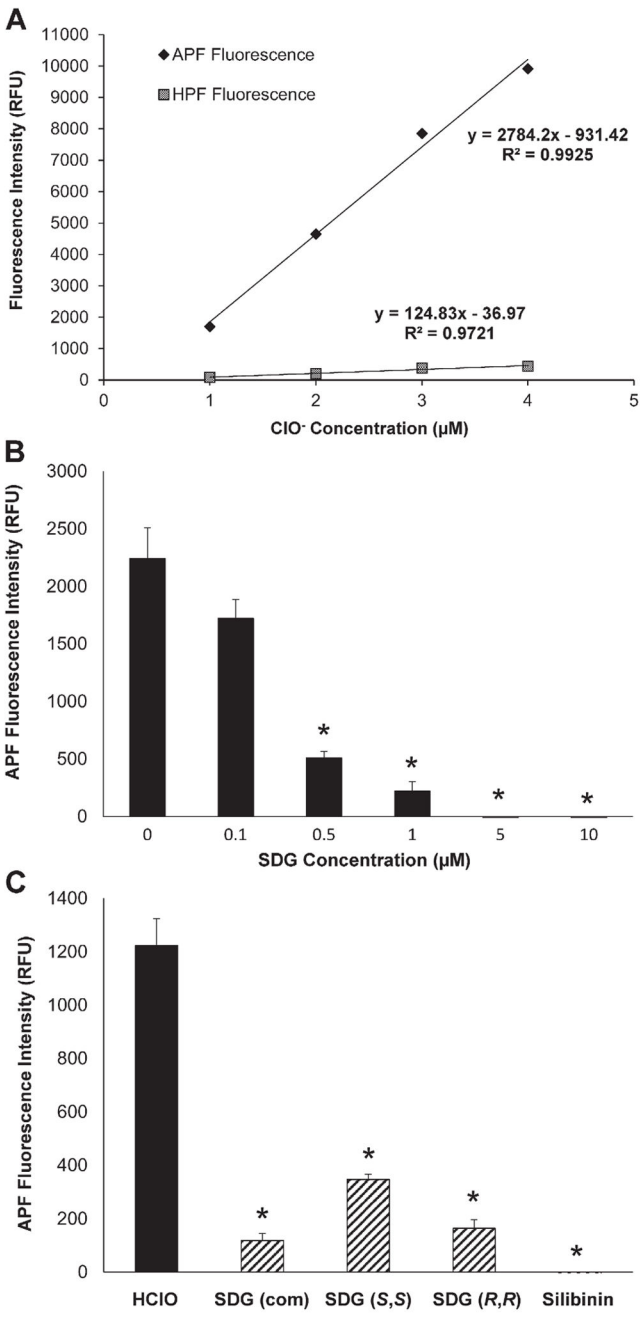

Fig. 3.

SDG scavenges hypochlorite ions Panel 3A shows the ClO^- dependent increase in APF and HPF fluorescence in PBS. Panel 3B shows scavenging of ClO^- by SDG. Panel 3C shows the scavenging effect (0.5 μM) of commercially available SDG (com), synthetic SDG diastereomers SDG (*S*,*S*) and SDG (*R*,*R*), and silibinin. All samples were evaluated in duplicate. The data are presented as mean + SEM. * indicates a statistically significant difference ($p < 0.05$) as compared to untreated control.

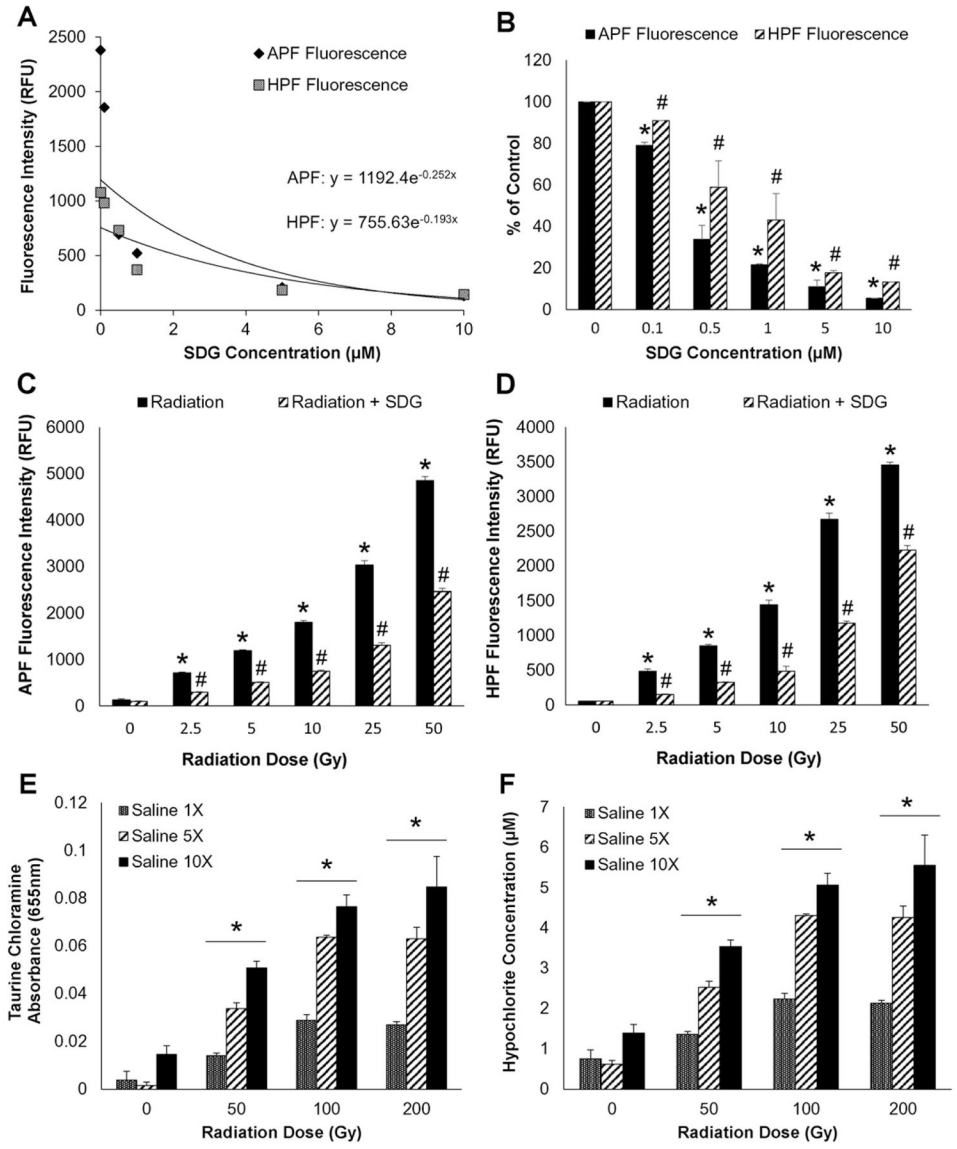

Fig. 4.

SDG scavenges γ-radiation-induced generation of ACS Panels 4A and 4B show the γ-radiation-induced (50 Gy) increase in APF and HPF fluorescence and the concentration-dependent, scavenging effect of SDG at various concentrations using APF and HPF fluorescence. Panels 4C and 4D show the scavenging effect of SDG on generation of ACS at increasing doses of radiation in PBS with either APF or HPF (see Fig. 3 legend). Panels 4E and 4F show γ-radiation-induced chlorination of taurine. Panel 4E shows the γ-radiation-induced taurine chloramine formation as absorbance at 655 nm under all experimental conditions. Panel 4F shows the hypochlorite concentration (μM) under various conditions as in Panel 4E. For Panels 4A–4B, all samples were evaluated in duplicate whereas for Panels 4C–4F, all samples were evaluated in quadruplets. The data are presented as mean + SEM. * indicates a statistically significant difference ($p < 0.05$) as compared to untreated control and

# indicates a statistically significant difference ($p < 0.05$) between respective SDG concentrations and radiation dose exposure groups.

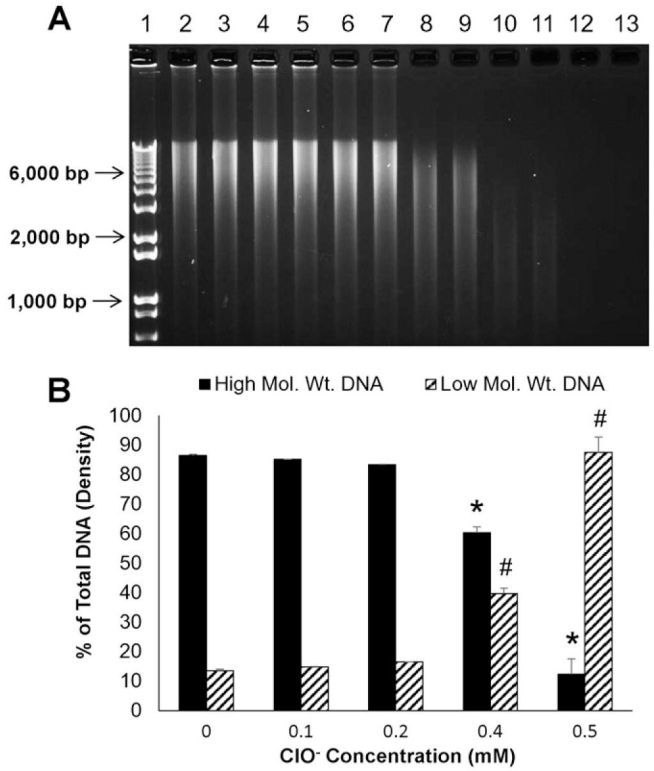

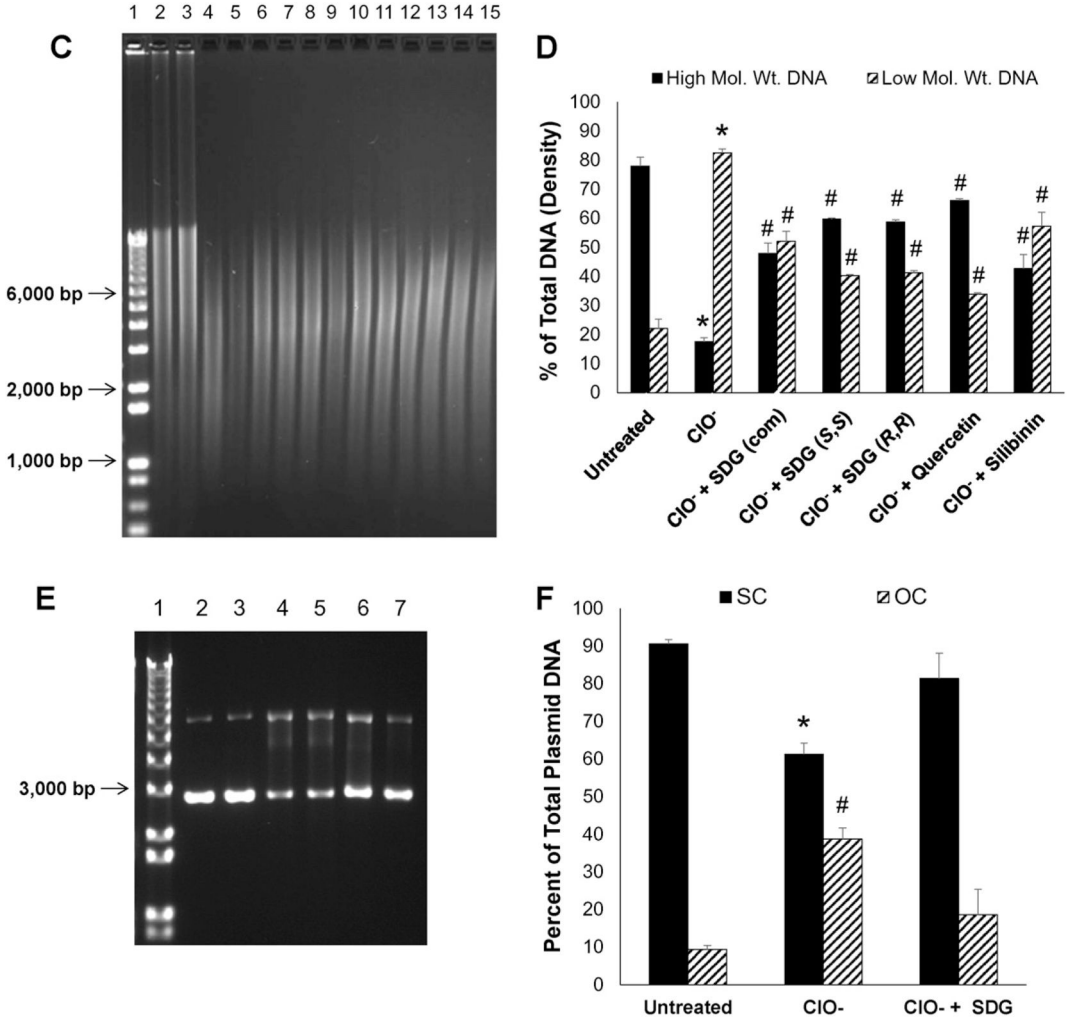

Fig. 5.

Hypochlorite-induced calf thymus DNA damage Panels 5A and 5C show representative agarose gel scans of calf thymus DNA following exposure to HOCl. Panels 5B and 5D show high and low molecular weight DNA fragments as percent of total DNA. Panels 5E and 5F show the effect of SDG on hypochlorite-induced damage to plasmid DNA. Panel 5E shows a representative agarose gel of plasmid DNA after exposure to HOCl. Panel 5F shows SC and OC forms presented as percent of total plasmid DNA. For Panel 5A, lane 1 — 1 kb DNA standard ladder, lanes 2 and 3 — untreated DNA, lanes 4 and 5 — 0.1 mM ClO^-, lanes 6 and 7 — 0.2 mM ClO^-, lanes 8 and 9 — 0.4 mM ClO^-, lanes 10 and 11 — 0.5 mM ClO^- and lanes 12 and 13 — 0.6 mM ClO^-. * indicates a statistically significant difference ($p < 0.05$) in high molecular weight DNA as compared to untreated control and # indicates a statistically significant difference ($p < 0.05$) in low molecular weight DNA as compared to untreated control. For **Panel 5C**, Lane 1 — 1 kb DNA standard ladder, lanes 2 and 3 — untreated DNA, lanes 4 and 0.5 mM ClO^-, lanes 6 and 7 — 0.5 mM ClO^- + SDG (com) 1 μM, lanes 8 and 9 — 0.5 mM ClO^- + SDG (*S,S*) 1 μM, lanes 10–11 — 0.5 mM ClO^- + SDG (*R,R*) 1 μM, lanes 12–13 — 0.5 mM ClO^- + quercetin 1 μM and lanes 14 and 15 —

0.5 mM ClO^- + silibinin 1 μM. * indicates a statistically significant difference ($p < 0.05$) in high and low molecular weight DNA as compared to untreated control and # indicates a statistically significant difference ($p < 0.05$) in high and low molecular weight DNA as compared to 0.5 mM ClO^-. For Panel 5E, Lane 1 — 1 kb DNA standard ladder, lanes 2 and 3 — untreated plasmid DNA, lanes 4 and 5 — 4.5 mM ClO^-, lanes 6 and 7 — 4.5 mM ClO^- + SDG 25 μM. The data are presented as mean + SEM. * indicates a statistically significant difference ($p < 0.05$) in SC DNA as compared to untreated control and # indicates a statistically significant difference ($p < 0.05$) in OC DNA as compared to untreated control.

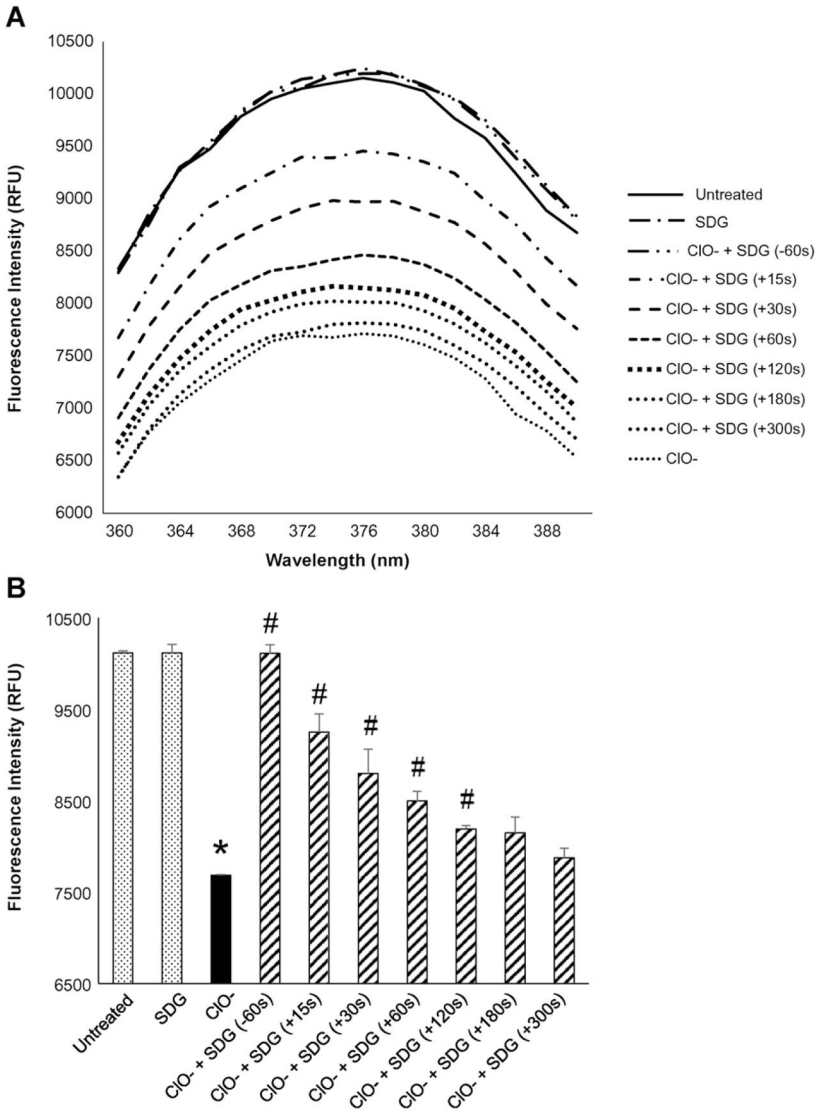

Fig. 6.

Effect of SDG (pre- and post-treatment) on hypochlorite-induced modification of 2-aminopurine (2-AP) Panel 6A shows the representative spectra for all the treatment conditions. Panel 6B shows the fluorescence at 374 nm (emission maximum) under different conditions as in Panel 6A. For each condition, all samples were evaluated in duplicate. The data are presented as mean + standard error. * indicates a statistically significant difference ($p < 0.05$) in fluorescence intensity as compared to untreated control and # indicates a statistically significant difference ($p < 0.05$) in fluorescence intensity as compared to ClO^{-}.

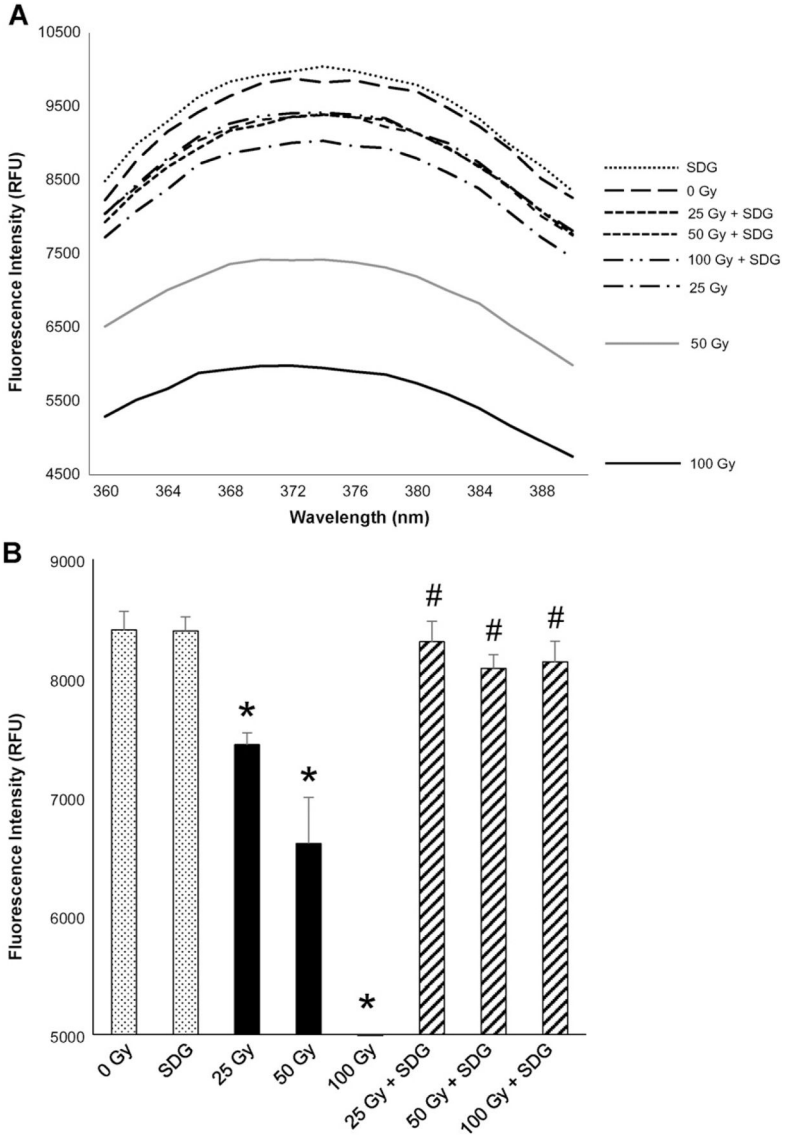

Fig. 7.

SDG prevents γ-radiation-induced modification of 2-aminopurine (2-AP) Panel 7A shows the representative spectra for all the treatment conditions. Panel 7B shows the fluorescence at 374 nm (emission maximum). For each condition, all samples were evaluated in duplicate. The data are presented as mean + standard error. * indicates a statistically significant difference ($p < 0.05$) in fluorescence intensity as compared to the 0 Gy treatment condition (control) and # indicates a statistically significant difference ($p < 0.05$) in fluorescence intensity as compared to each respective radiation dose treatment condition.

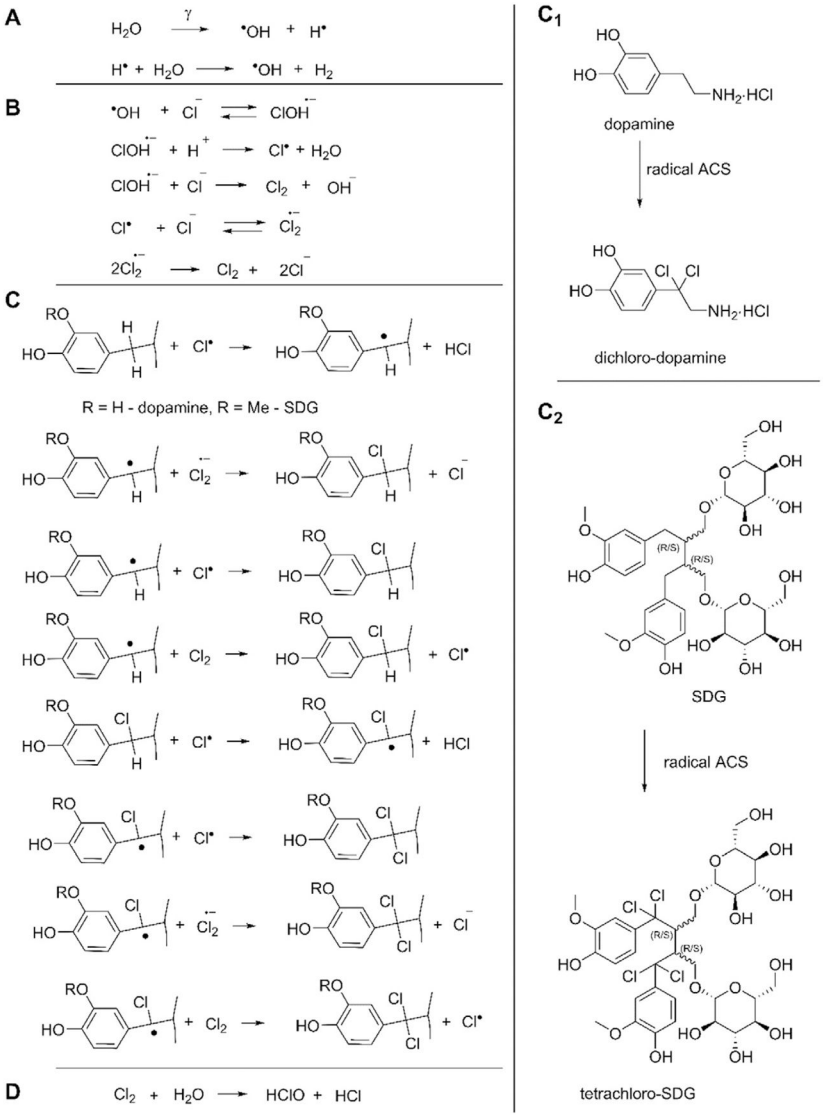

Scheme 1.

Reactions of active chlorine species produced by γ-irradiation of physiological solutions - chlorination of dopamine and SDG. A possible mechanism of radical chlorination of dopamine and SDG is presented in Scheme 1. Panel A shows a simplified process that one γ-photon can produce two hydroxyl radicals. Panel B shows the formation of ACS. Panel C and C_1 show that dichloro-dopamine molecules are produced with four chlorine atoms. Panel C and C_2 show the formation of tetrachloro-SDG as it contains two benzyl moieties. Panel D shows that HOCl/ClO^- are secondary ACS formed by disproportionation of Cl_2.

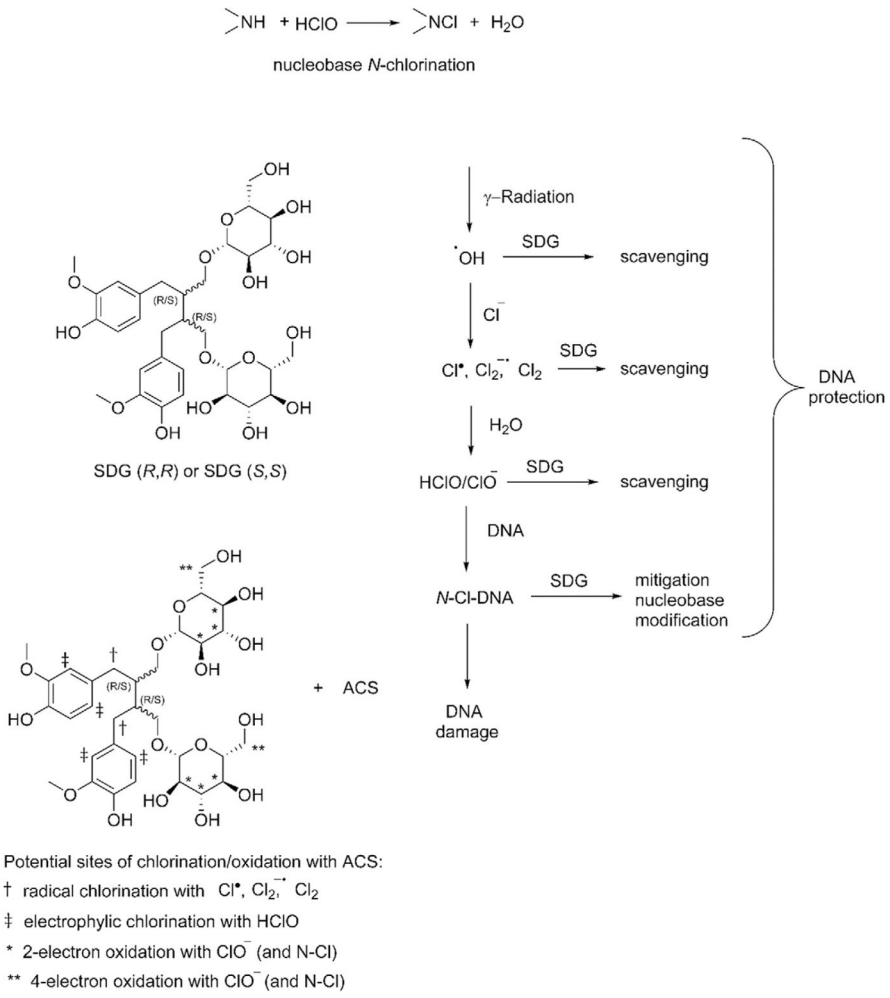

Scheme 2.

Proposed mechanism of SDG action in DNA protection from nucleobase chlorination SDG prevents and mitigates radiation-induced DNA damage in PBS by scavenging hypochlorite ions (ClO^-) and reducing chlorinated nucleobases.